

## Validation of TSP measurements for the stall behavior of a NACA-0012 airfoil with LDV

### Validierung von TSP Untersuchungen zum Ablöseverhalten am Beispiel eines NACA-0012 Profils mittels LDV

**Michael Dues<sup>1</sup>, Jonas Johannes Steinbock<sup>1</sup>, Adi Siswanto<sup>1</sup>, Sergey Melnikov<sup>1</sup>, Fabian Rohr<sup>2</sup>, Michael Schäferling<sup>2</sup>, Peter Guntermann<sup>3</sup>, Harry Hayer<sup>3</sup>**

1) ILA R&D GmbH (ILA), Jülich, Deutschland

2) FH Münster (FHM), Münster, Deutschland

3) European Transonic Windtunnel (ETW), Köln, Deutschland

Key words: LDV, TSP, PSP, Stall, NACA 0012

Schlagworte: LDV, TSP, PSP, Ablösung, NACA 0012

#### Preface

This version has been translated from the german version with the aid of the software gpt4all by nomic-ai using the Mistral-OpenOrca model, see also <https://www.nomic.ai/gpt4all>.

The original german version can be found at:

<https://www.gala-ev.org/images/Beitraege/Beitraege2025/pdf/4.pdf>

#### Abstract

In this article, temperature sensitive paint measurements are presented for visualizing stall condition and the transition from laminar to turbulent boundary layer flow over a flat plate and on NACA 0012 profiles [1]. The flow condition is verified by LDV measurements.

#### TSP Experiments at ETW

In this context, temperature sensitive paint (TSP) is primarily used to determine the laminar-turbulent transition on the surface of aircraft models, see [2]. Knowledge about this process is a prerequisite for developing fuel-efficient airplanes that rely on sustaining laminar flow as much as possible.

Even though numerical simulations of transonic aircraft flow have made significant progress in recent decades, experimental investigations are still needed, especially in parameter ranges where the physical processes are non-linear, such as separation, transition or interaction between shock and laminar boundary layers. These effects depend on the boundary layer thickness/Reynolds number. Therefore, experimental studies should be mechanically similar (i.e., at flight-relevant Reynolds numbers) and can only be carried out in wind tunnels with reduced scale aircraft models under cryogenic conditions. Currently, there are only two wind tunnels worldwide capable of this [3]. One of them is the European Transonic Wind Tunnel (ETW) in Cologne, which can realize temperatures down to -160°C and pressures up to 4.5 bar.

In experimental investigations in the ETW, increasingly optical measurement techniques are being used, such as TSP (temperature sensitive paint) and PSP (pressure sensitive paint) since they have the fundamental advantage of being non-invasive or minimally invasive and therefore do not disturb the flow under investigation. In addition, only minor modifications are

required for the model, such as applying a sensor layer or marker points, which offers advantages for scaled models.

In free flight and conventional wind tunnels, the location of the laminar-turbulent transition is often determined using an IR camera, which is not possible in a cryogenic wind tunnel like the ETW due to low temperatures. By the increased heat exchange in a turbulent boundary layer compared to a laminar one, a temperature distribution on the model surface can be visualized. The transition is then identifiable by a clear light-dark contrast. The TSP measurement technique used in the ETW was developed in cooperation with DLR in Göttingen (Institut für Aerodynamik und Strömungstechnik) as well as the University of Hohenheim and later FH Münster, and adapted for cryogenic applications [4], [5], [6], [7].

TSP was further developed for use in the ETW in various LUFO and EU projects, such as ALSA, ReSK, LoCaRe, BinCola [8], HiLamBiz [9], NLF-WingHiper [10]. Some examples of this are shown in Figure 1.



Figure 1: Temperature sensitive paint-coated models in the ETW. Top left: Full model (EC FP7 HiLamBiz). Bottom left: Full model (LuFo V-2 ReSK). Right: Half model (LuFo IV ALSA).

Today, TSP is standardly used in the ETW as a measurement technique for locating the transition for all laminar tests. While initially requiring a small temperature difference between the model and fluid to be realized through a minimal temperature jump of the incoming flow, developments have been made with heating the sublayer within the TSP coating (carbon nano tubes, CNT) [6], [11]. Nowadays, heating is mostly done using a high-power diode laser in the infrared range (IR), which warms up the entire model surface by just a few degrees Kelvin. This power is transmitted through an optical fiber into the low temperature pressure chamber of the wind tunnel and focused onto the model surface via a beam forming optics. The laser

source can therefore be operated outside of the wind tunnel, simplifying operation or even making it possible in the first place. The high intensity of the heat radiation combined with a powerful lighting system to excite TSP molecules as well as a corresponding high-speed camera allow for dynamic measurements in the kHz range, which are increasingly needed for aeroelastic investigations.

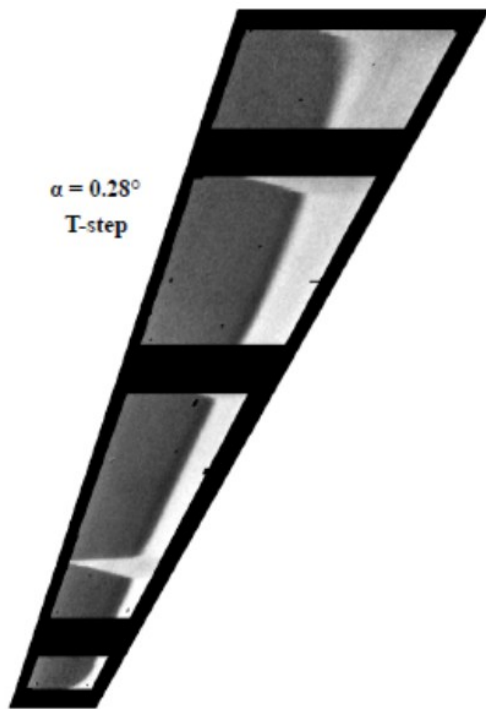


Figure 2: Visualization of the laminar-turbulent transition on a forward swept wing configuration NLF Ecowing FSW (LuFo project ULTIMATE) at an angle of attack of  $0.28^\circ$ . Flow direction from left to right. The darker area corresponds to a laminar boundary layer, lighter areas are turbulent.

Recent developments are moving towards estimating the wall shear stress distribution on the wing surface using TSP-measured temperature gradients and a subsequent CFD approach. This would then correspond to a virtual oil streak that is not dirtying, reproducible, unsteady, and quantifiable.

Other interesting developments for ETW are the combination of temperature and pressure sensitive paint as well as standardization of required hardware and software, which is also addressed in the ZIM project KoMeTD.

### Temperature-sensitive Paints

Coatings with temperature-sensitive paint (TSP) are the basis for imaging methods, allowing experimental determination of temperature distributions on a surface without influencing the investigated model surface. TSPs enable continuous measurement and visualization of flow and temperature fields with high spatial resolution. This allows quantitative determination of heat transfer on test bodies and model surfaces. Thus, visualizing an important parameter in fluid mechanics: the laminar-turbulent transition in wind tunnel models.

TSPs are polymer-based paints in which temperature-sensitive photoluminescent dyes are embedded. With increasing temperature, the quantum yield of the dyes and thus the intensity

of luminescence decrease, as the probability for non-stimulated transitions from electronically excited states to the ground state increases (thermal quenching). The relationship between intensity  $I$  and absolute temperature  $T$  can be represented by the Arrhenius equation (Equation 1) [12].

$$\frac{I(T)}{I(T_{ref})} = \frac{E_{nr}}{R} \left( \frac{1}{T} - \frac{1}{T_{ref}} \right) \quad (1)$$

with  $E_{nr}$  = activation energy of the non-stimulated transition,  $R$  = general gas constant and  $T_{ref}$  = reference temperature in K. A representation of the relationship between temperature and intensity is given in Figure 3.

The analytical temperature sensitivity is the relative change in luminescence intensity per degree Kelvin. Temperature differences can be determined using TSPs with an accuracy of 0.2-0.8K [12].

As temperature-sensitive dyes, europium or ruthenium complexes with organic ligands are often used [13]. The latter can also be used for fluid mechanics measurements in the cryogenic temperature range [14]. The dyes are mixed with a suitable solvent containing a polymer binder to form a sprayable solution. Common polymer materials are polystyrene, polymethyl methacrylate, polyurethane or epoxy resins. After spraying the paint mixture, the solvent evaporates and leaves a homogeneous film on the surface with a thickness typically between 10 and 50 nm. Various substrates can be coated in this way, such as stainless steel, aluminum, or plastics.

In this project, we use a europium complex with Dithienylpropandion ligands as the temperature-sensitive dye, whose luminescence can be excited by a blue 405 nm LED light [15]. The intensity of the red emission band of europium with a maximum at 612 nm is used as the temperature-sensitive signal (Figure 3). A two-component polyurethane is used as the polymer binder.

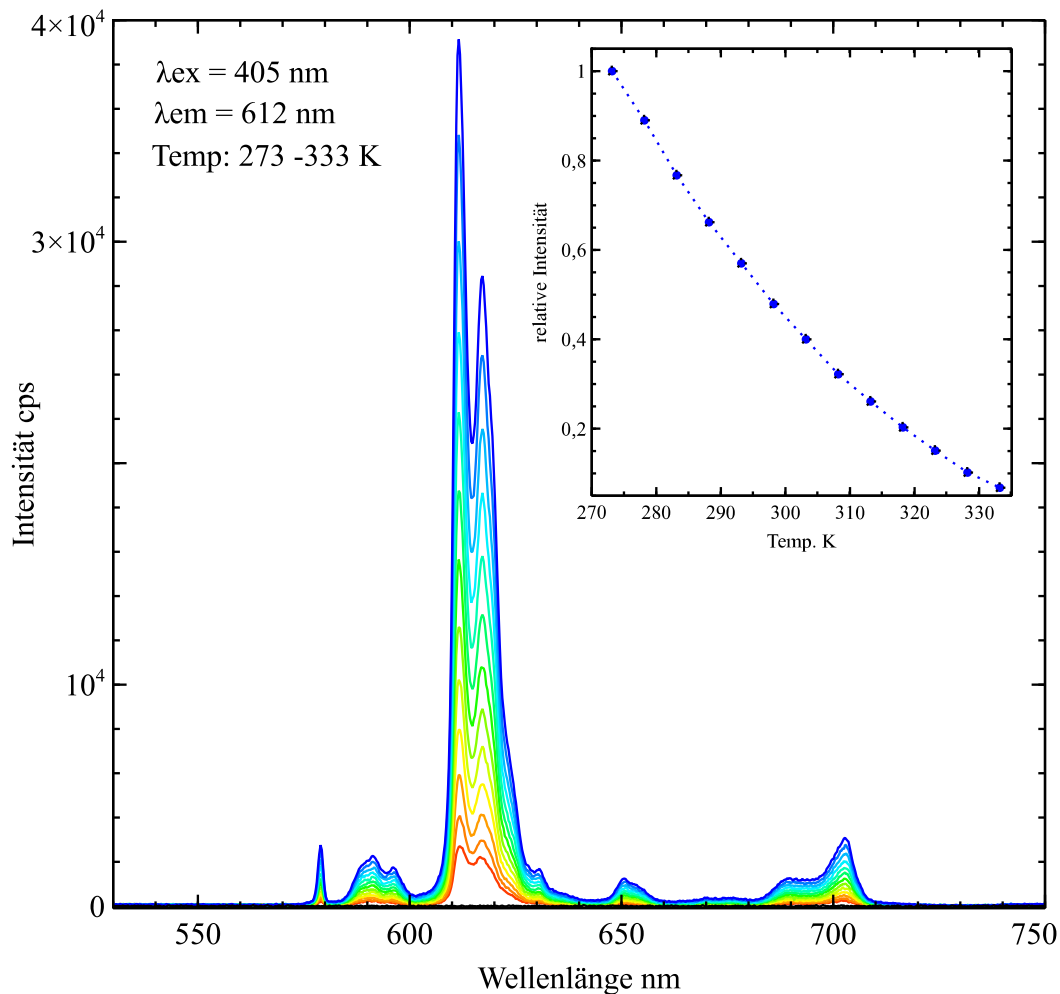


Figure 3: Temperature-dependent luminescence spectra of the TSP coating after 24h drying (average film thickness: 20 $\mu$ m) on aluminum with a polyurethane primer. The temperature sensitivity at 30°C is 4.1%/K. The blue line represents the spectrum at 273 K, and the red one at 333 K. On the top right, an insert shows the representation of the (integrated) relative intensity versus the temperature in Kelvin.

### Assembly of the TSP System

In this chapter, the components of the system, the measuring process, the acquisition mode and the evaluation algorithm for TSP/PSP measurements are outlined.

#### Components

The TSP/PSP measurement system consists of the following core components: sensor (TSP dye), lighting unit, synchronization unit, camera, and evaluation software. The test object (here: airfoil) must be suitable for coating with the TSP dye. The measurements shown were carried out using 3D printed thermoplastic airfoils that were coated with the TSP/PSP color by FHM using a spray method. As a lighting unit, a modular LED unit (ILA R&D GmbH) is used. This lighting unit stands out for its short fall times (<100 ns) and high light intensity. The PSP dye is excited with a 405 nm LED array. The LED array has a power of 12W (cw). In pulsed operation, significantly higher power operation are possible. The effective maximum power for the pulse mode is essentially limited by the cooling of the LED.

The LED module allows for quick exchange of the LEDs, for example to adapt to another wavelength. Up to four LEDs/LED arrays can be controlled in parallel or individually. The

parameterization and temporal sequence between lighting and camera are realized by a microcontroller-controlled synchronization unit. Optocouplers for the four digital input and output signals enable the application of the sequencer in industrial environments. The smallest adjustable time difference is 1  $\mu$ s. The shortest trigger time is 10  $\mu$ s.

The utilized global shutter camera (Backside Illuminated CMOS) allows frame rates of 55 Hz with a discretization of 12 bit at 2064x1544 pixels. At 8 bits, 115 Hz are possible. The pixel size is 3.45 x 3.45  $\mu$ m. The Quantum Efficiency is specified as 65% at 532 nm.

The camera has a configurable output signal that can be synchronized with the active camera capture. This allows for documenting the actual time or time difference of the acquisition(s). Exposure times range from 1  $\mu$ s to 30 s. Noteworthy is that the camera also features a "multiple exposure" mode, allowing measurements even at very weak signals (with reduced temporal resolution) to be carried out.

### **Measurement Procedure**

TSP measurements document the surface temperature of the measurement object, usually referenced to a known reference condition. Fluid processes such as laminar/turbulent boundary layer transition or flow separation lead to significant changes in surface temperature due to changing heat transfer. This effect can be significantly amplified by increasing the temperature difference between the fluid and the measurement object through heating/cooling of the fluid or the surface.

It is therefore usually useful to temper the measurement object (airfoil / model) or the flow. For the measurements in question, the object is heated with an infrared lamp to about 70°C, with a temperature of the fluid at around 18-20°C. Tempering takes place before each measurement without flow and with open window. After successful tempering, the window is closed and TSP measurements are taken.

For each measurement campaign, in addition to the actual signal images (tempered airfoil, color excitation with LED), dark images (camera closed) and environmental images (measurement conditions without LED) are also recorded. For the images shown here, the activation of the TSP color is pulsed with a constant frequency in the range of 15-30 Hz. The acquisition of TSP images takes place approximately 10  $\mu$ s after switching off the LED in the area of the decaying emission. In this way, it is possible to perform TSP measurements without special bandpass filters.

### **Acquisition Modes**

Conventional cameras take images in "single exposure" mode, which means that the photoactive surface on the camera chip (CMOS or CCD) is exposed once. After synchronous exposure, analog-to-digital conversion and data reading takes place. For the single exposure mode, the exposure time is chosen so that the strongest expected signal corresponds to about 75% of the possible pixel values (4096). The intensity of the signal from TSP/PSP measurements depends on factors such as the dye, coating, thickness of the coating, exposure intensity, excitation wavelength, temperature and pressure. The light emitted by the TSP/PSP dyes (signal) is limited to a relatively short time window after successful activation. If it is not possible to increase the signal intensity by extending the camera's exposure time, the camera can sum up weak signal levels to a desired signal level in multiple exposure mode. The height of the effective signal level can be set by the number of repetitions (exposure). Signal summation takes place directly on the camera chip; the cumulative signal image is then read out as a combined image. By using "multiple exposures" measurements can also be

performed at very low signal levels. The signal-to-noise ratio (SNR) remains almost constant with for the effective exposure time, compare Fig. 4 (right), and Eq. (2). The effective SNR for the examined generic images on a pixel basis - independent of the number of exposures - is essentially a function of local signal intensity.

$$SNR_{dB} = 10 \cdot \log_{10} \frac{\mu_{pxl}}{\sigma_{pxl}} \quad (2)$$

with  $\mu_{pxl}$  = mean and  $\sigma_{pxl}$  = standard deviation of the pixel intensity for a series of images.

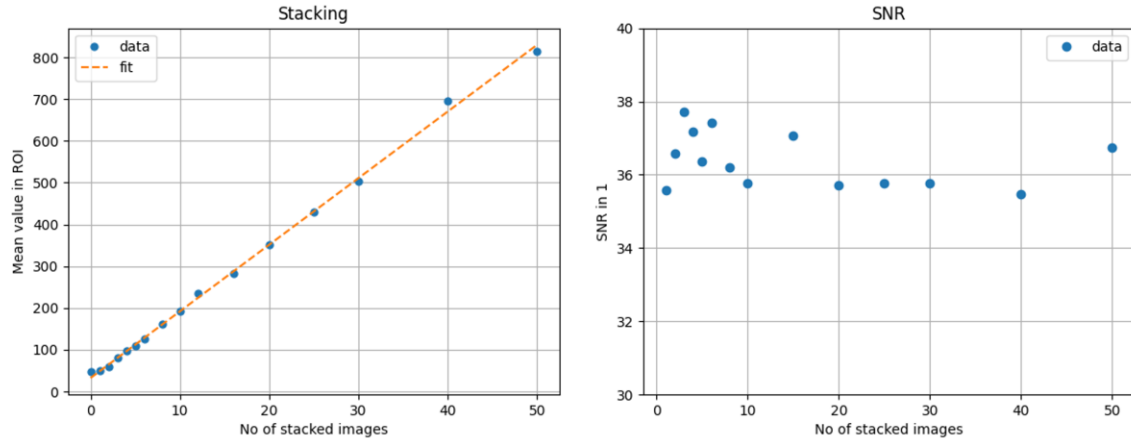


Figure 4: Left: Measured average intensity plotted over the number of exposures with a constant single exposure time of 200 $\mu$ S. Right: Average SNR plotted over the number of expositions with a constant effective exposure time of 50 ms.

During one measurement series, the settings for exposure time, number of exposures and amplification are kept constant.

### Evaluation algorithm

In TSP/PSP measurements, the measured property of intensity (counts or pixel value) is linked over a calibration with measurement quantities (temperature/pressure). The calibration curve is shown in Figure 3 (inserted above right), generated from the respective luminescence spectra.

The intensity is normalized by the intensity at a known reference condition (temperature/pressure). Subsequently, the curve is approximated using a least square calculation to obtain a calibration function. In this case, a polynomial function was used because it better approximates the measurement data than the physically based Arrhenius equation, see Equation (1).

To determine the surface temperature from the intensity values, the actual measured signal is then subtracted by background and dark noise. To eliminate uneven illumination, the measured signal is divided by the corrected reference image. Based on this relative image, the surface temperature can be determined taking into account the calibration. Pixels whose intensity or temperature values are located outside the calibrated range are excluded from further evaluation.



## Assembly of the experiment

In this section, the setup of the experimental facility, the characterization of flow conditions using LDV (Laser Doppler Velocimetry), and the investigated airfoil models are described.

### Testrig/ LDV

The test stand consists of an open wind tunnel with conditioned inflow. The wind tunnel is driven by a fan in suction configuration. Following the inlet nozzle, there is conditioning of the inflow through several strainers and subsequent narrowing of the flow cross-section, see Figure 5. The cross-section of the square test chamber is 70 x 70 mm. The maximum wind tunnel speed in the measurement section is 100 m/s. The flow in the test chamber can be observed through windows on up to four sides. Lateral insertions allow for positioning of the airfoil profiles at angles relative to the inflow between 0° and 15°.

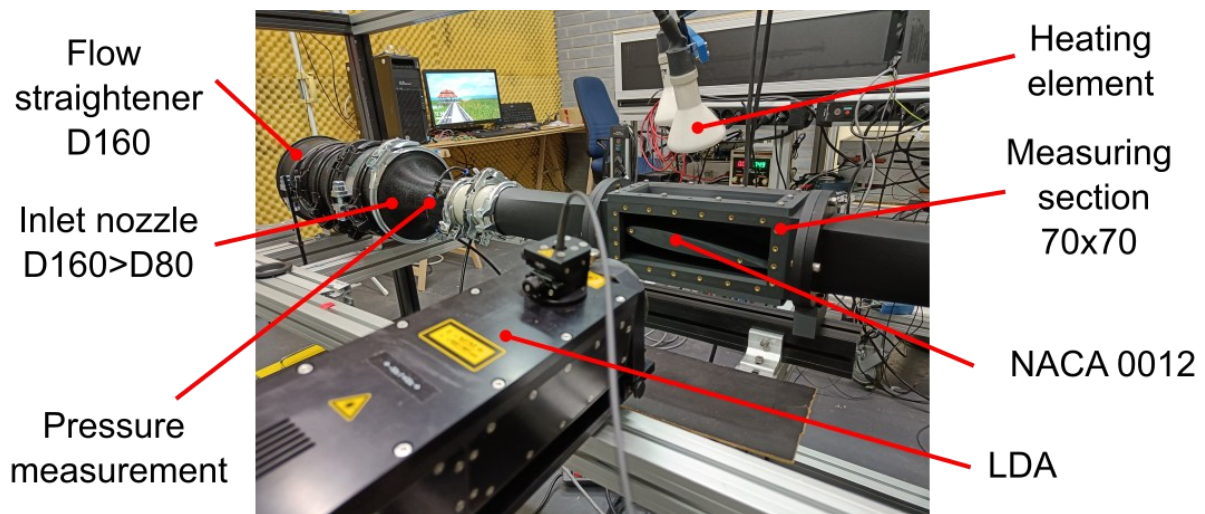


Figure 5: Test stand with LDV probe in the foreground, open test chamber with NACA profile. Flow direction from left to right. Camera and LED lighting from above (not shown).

### Characterization of the inflow

For the characterization of the incoming flow of the empty test chamber, a newly developed industrial non-shifted LDV probe (iLDV) is used. The wavelength is 532 nm (Nd:YAG), and the used focal length is 250mm.



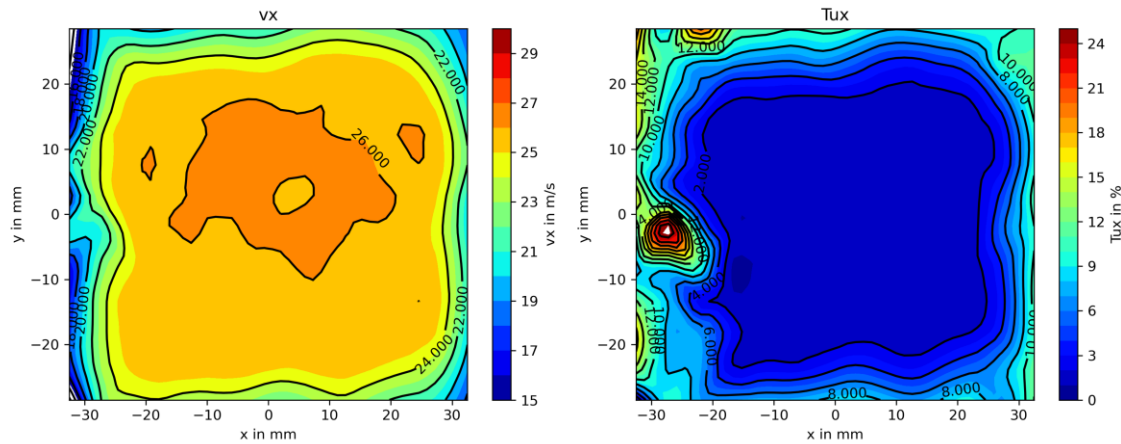


Figure 6: Left: Contour plot of the axial velocity over the square measurement cross-section (without installed airfoil) for a grid of 168 measurement points. The plateau in the middle is approximately at 25 m/s. Right: Plot of corresponding 1D turbulence level in %. The central plateau is approximately at 2%.

The wind tunnel is operated at 30% of its maximum speed. Within the square test chamber, a region of homogeneous core flow forms in which the velocity is approximately 25 m/s and the axial turbulence grade is about 2%. The core flow extends over an area of about  $\pm 25$  mm relative to the center of the cross-section. The first TSP measurements will be carried out in this area. At the edges of the wind tunnel, boundary layers with a thickness of approximately 10 mm form, see Figure 6. Due to optical access, the measurement grid ends vertically (y-axis) at  $\pm 30$  mm.

### Investigated Airfoils

As a pre-study for the measurements shown in this paper, a flat plate (thickness 8 mm) with applied cylindrical disturbances (diameter 1 mm; height 0.5 mm) was investigated. The disturbances were placed at distances of 19, 24 and 29 mm from the front edge as well as at a distance of 15 mm from the midline. The flat plate is rounded off at the front ( $R=4$ mm), while it extends over a length of 20 mm in a conical shape at the rear. The width of the flat plate corresponds to the channel width of 70 mm. The axial length is 66 mm.

Furthermore, a NACA 0012 profile without disturbances and one with applied cylindrical disturbances (diameter 1.5 mm; height 0.5mm; at distances of 30, 60 and 90 mm from the front edge; distance of 15 mm from the profile center) were investigated, see Figure 7. The NACA 0012 profile has an axial length of 200 mm.

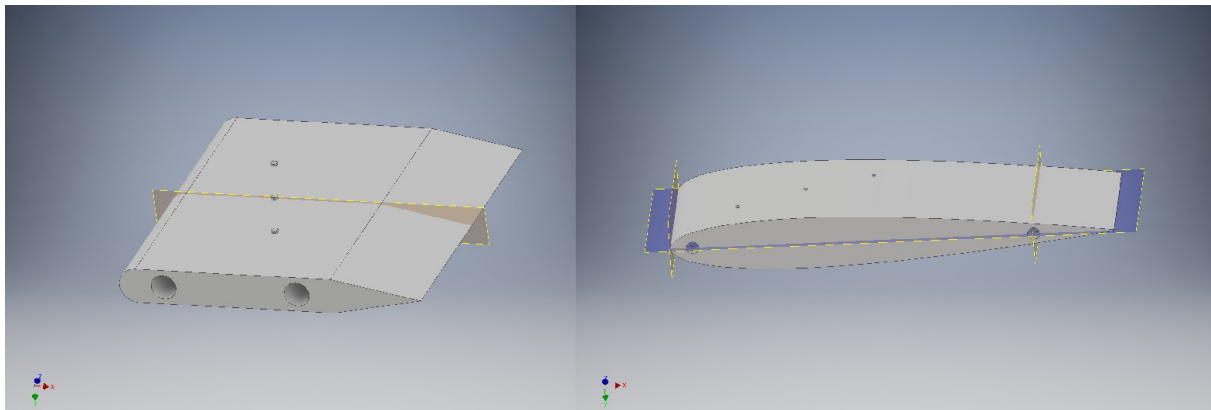


Figure 7: Left: 3D CAD view of the flat plate with a length of 70 mm. Right: 3D CAD view of the NACA 0012 profile with a length of 200 mm. The images are not to scale.

## Results

In this section, the results of the measurements on the flat plate and the NACA 0012 profile are presented.

### Flat plate with disturbances

The preliminary investigations are carried out on a flat plate with an angle of attack of  $0^\circ$ , where the imposition of three cylindrical disturbances on the surface causes a flow separation, see Figure 7 (left).

TSP measurements on the flat plate show a decrease in surface temperature behind the disturbances, which is caused by an increase in heat transfer at the profile surface due to the cross-flow exchange during the flow separation, see Figure 8.

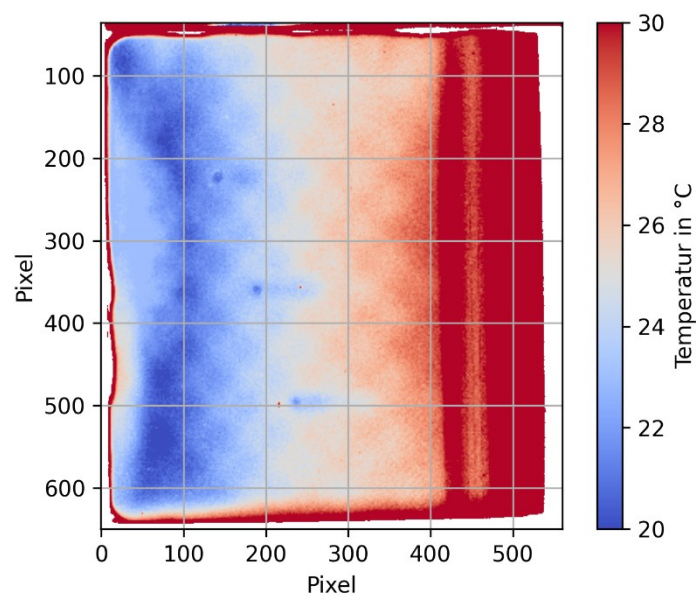


Figure 8: TSP measurement of the flow separation on a flat plate at 30 m/s. Flow direction from left to right. The preheated profile is already cooled at the front edge. The Reynolds number is  $1.3e^5$ . Areas that are white are outside the calibration range of the TSP color.

Further, the TSP technique makes the internal support structure of the flat plate (3D print) visible. Due to the Reynolds number of  $1.3e^5$ , the flow would be described as laminar. The measurement shown in Figure 8 was carried out with an existing commercial color camera with limited temporal resolution and configurability within the scope of preliminary investigations. For further investigations on the NACA profile, a camera adapted to the requirements of steady-state TSP/PSP measurements was used.

The change in flow structure at the disturbance location on the flat plate is confirmed by qualitative changes in the axial velocity profiles, see Figure 9 (left). The velocity profiles were recorded with an unshifted iLDV system.

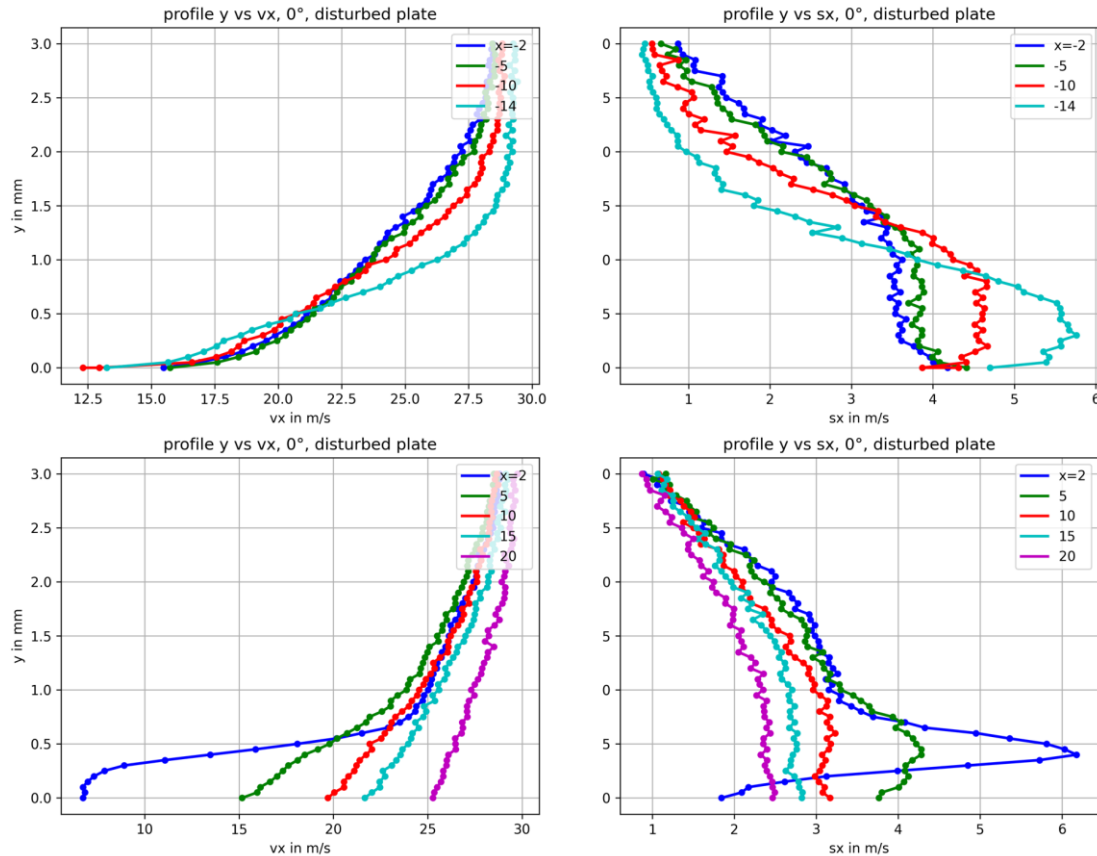


Figure 9: Top: Upstream flow. Bottom: Downstream of the disturbance. Left: Plot of absolute axial velocity  $v_x$  over distance to surface  $y$  at different horizontal distances from the first obstacle on the surface. A negative number means that the position is streamwise up to the first applied disturbance. Right: Fluctuation speed (standard deviation). The zero point for the distance to the profile surface (horizontal axis) corresponds to the traversal coordinates and is approximately 0.1mm above the flat plate's surface. The LDV measurements were carried out at lowest disturbance shown in Figure 8.

The flow changes its characteristics during the separation of the flat plate. Streamwise, an approach to a turbulent profile form can be observed, see Figure 9 (top left). The course of the fluctuation magnitude as in Figure 9 (top right) depicted, indicates that a laminar turbulent transition is currently taking place (-14 [cyan]). Correspondingly, a local temperature drop can be detected in Figure 8 at a horizontal position of about 100 pixels. Directly after the disturbance location, a velocity profile characteristic for a flow separation occurs (Line 2 [blue], bottom). The fluctuation magnitude also shows a maximum at Line 2 [blue], see Figure 9 (right, bottom).

The reattachment flow in the separation cannot be resolved with an unshifted LDV system due to system limitations. Therefore, a LDV system with direction detection is used for the investigations on the NACA 0012 profile. For the following LDV measurements on the NACA profile, the LDV rays were aligned parallel to the wall surface in order to be able to measure as close to the wall as possible when performing the profile. The first measurement point is approximately 0.05 mm away from the profile surface. Thus, the wall-conforming flow component is depicted.

#### **NACA 0012 with an angle of attack of $7.5^\circ$ with wire**

In this section, experiments on the visualization of an enforced laminar-turbulent transition in the reattachment of a flow over a  $7.5^\circ$  NACA 0012 profile are discussed.

As shown in Figure 10 (top), the temperature in the wake of the wire, which extends across the upper half of the profile width, is significantly reduced due to turbulence excitation. Around 20 mm, the dampening influence of the tesafilm ® on heat exchange can also be clearly observed.

Figure 10 (bottom left) shows the development and growth of the boundary layer in an undisturbed axial course. Very close to the leading edge (40 mm, blue line), the boundary layer profile exhibits a typical laminar behavior. Further downstream, the profiles become increasingly flat.

Figure 10 (bottom right) shows a local significant increase in fluctuation magnitude 40mm behind the entry edge, indicating a laminar/turbulent transition of the boundary layer. As the flow length progresses, the area of increased fluctuation magnitude spreads across the entire boundary layer height.

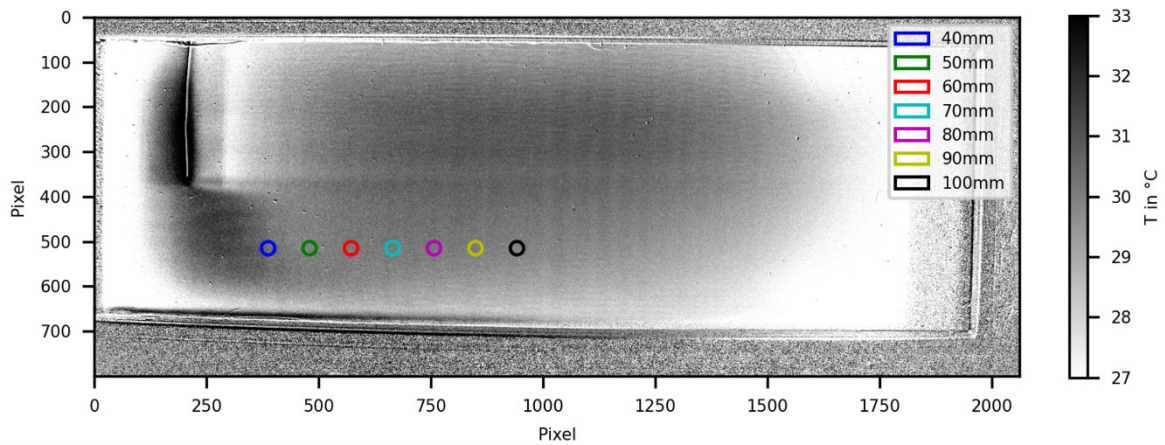


Figure 10: Top: TSP measurement of the NACA 0012 profile at an angle of  $7.5^\circ$  with a wire attached. Flow direction from left to right. The wire (0.25 mm) is glued with tesafilm® at an axial position of 20 mm, covering approximately half of the profile width. The centers of the colored circles mark LDV measurement positions. Dark areas correspond to higher temperature. Bottom left: Plot of wall coordinate  $y$  over the profile-conforming axial velocity  $v_x$  for measurement positions in the range of 40 to 100 mm downstream of the entry edge of the profile. Bottom right: Plot of wall coordinate  $y$  over the standard deviation of the axial velocity,

#### NACA 0012 with an angle of attack of $5^\circ$ with disturbances

In the following, experiments on visualizing an enforced transition in the boundary layer of a flow over a  $5^\circ$  NACA 0012 profile are discussed. To do this, cylindrical disturbances were applied to the wing contour, as shown in Figure 7 (right).



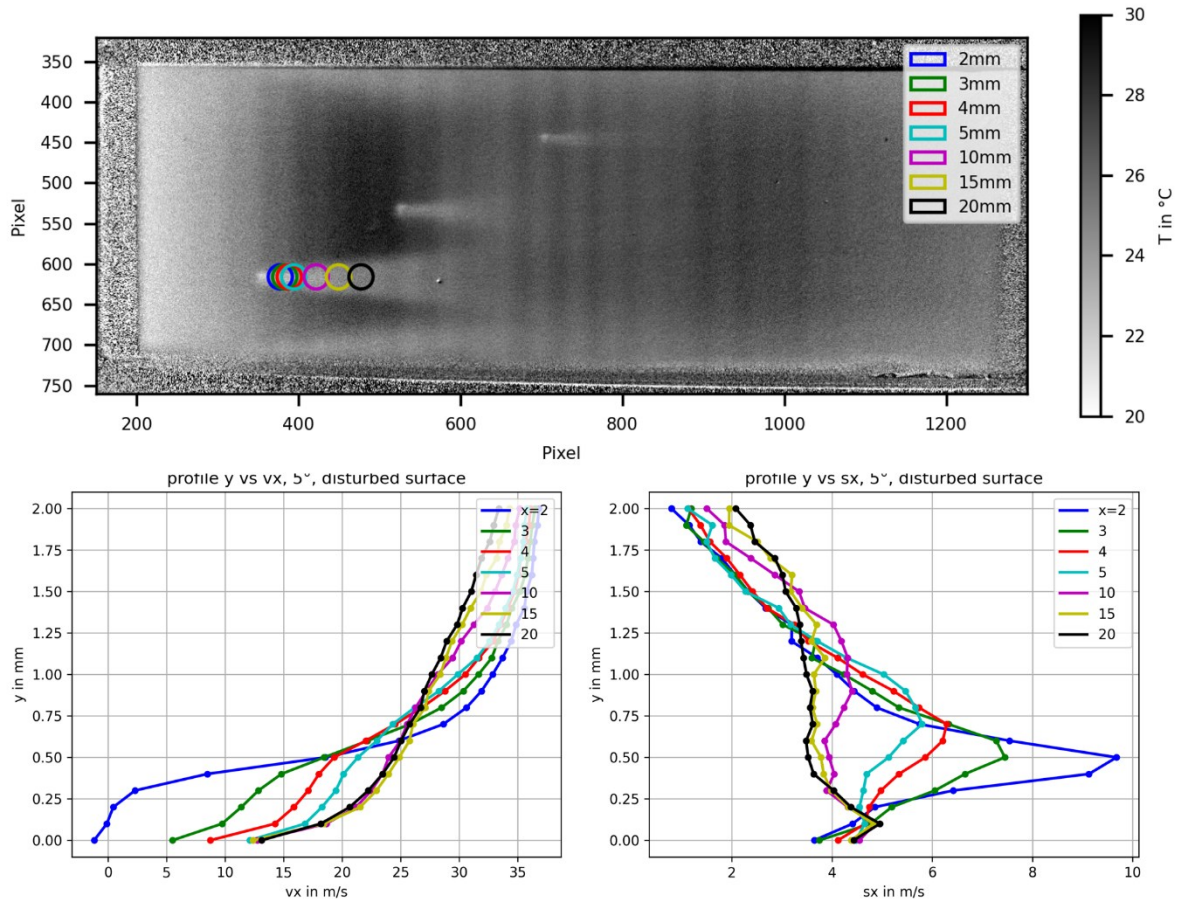


Figure 11: Top: TSP measurement of the NACA 0012 profile at an angle of  $5^\circ$  with three disturbances  $d=1.5\text{mm}$ . Flow direction from left to right. The colored circles indicate the LDV measurement positions, with the distance from the leading edge. Dark areas correspond to higher temperature. Bottom left: Plot of wall coordinate  $y$  over the axial velocity  $v_x$  for measurement positions in the range of downstream disturbance wake. Bottom right: Plot of wall coordinate  $y$  over the standard deviation of the axial velocity.

Figure 11 (top) clearly shows the separation areas with typical downstream cones behind the three applied disturbances. The LDV measurements in Figure 11 (bottom) are carried out in the wake of the leading disturbance. The separation behind the disturbance body can be identified on one hand by the form of the velocity profiles and, on the other hand, by the reverse flow zone ( $v_x$  negative). At the same time, the fluctuation speed increases significantly there.

## Conclusion

The presented investigations show that the TSP method is suitable for visualizing flow processes such as laminar/turbulent transition in the boundary layer or detecting separation areas. Compared to classical paint experiments, no contamination of the wind tunnel occurs. In addition, the TSP method can also be used for investigating unsteady phenomena.

The presented investigations show that LDV and TSP measurements complement each other. Together, they enable a coherent image of the boundary layer flow and allow the identification and assignment of effects such as separation and transition.

## **Outlook**

It is planned to expand the existing measurements with PSP measurements (pressure sensitive paint). This would then allow additional stagnation points and pressure gradients over the profile surface to be visualized. Based on preliminary investigations, a lower signal level can be expected in PSP measurements than in the TSP measurements presented here. Therefore, further studies are planned to optimize the possible TSP/PSP signal levels, for example by adjusting the time shift between excitation and exposure as well as selecting adapted bandpass filters.

Currently, the measurement object is preheated before carrying out the measurements and cools down during the course of the measurements due to the inflow and convection. Therefore, a continuous, adjustable heating system should be integrated into the measuring system in order to enable stationary measurements, longer effective measurement times, and shorter preparation times.

Furthermore, studies at higher speeds are planned. Based on TSP results from the ETW it is expected that different flow characteristics will distinguish themselves more clearly from one another at a higher Reynolds numbers.

## **Synopsis**

The flow phenomena of separation and laminar-turbulent transition were investigated using TSP measurements on laminar boundary layer NACA 0012 profiles as well as a flat plate. Artificial disturbance particles were applied to induce boundary layer transition or detachment of the flow. In the wake of the disturbance particles, areas with reverse flow, separation, or turbulent inflow can be visualized using TSP on the surface.

Complementary LDV measurements, which resolve the velocity direction, allow for secure assignment and interpretation of local flow conditions.



## Literatur

- [1] E.N. Jacobs, K.E. Ward, R.M. Pinkerton, The characteristics of 78 related airfoil sections from tests in the variable-density wind tunnel, NACA Technical Report (1933). <https://ntrs.nasa.gov/citations/19930091108>.
- [2] U. Fey, R.H. Engler, Y. Egami, Y. Iijima, K. Asai, U. Jansen, J. Quest, Transition detection by temperature sensitive paint at cryogenic temperatures in the European Transonic Wind tunnel (ETW), in: 20th International Congress on Instrumentation in Aerospace Simulation Facilities, 2003. ICIASF '03., IEEE, 2003: S. 77–88. <https://doi.org/10.1109/iciasf.2003.1274855>.
- [3] J. Green, J. Quest, A short history of the European Transonic Wind Tunnel ETW, *Progress in Aerospace Sciences* 47 (2011) 319–368. <https://doi.org/10.1016/j.paerosci.2011.06.002>.
- [4] K. Asai, R. Engler, J. Quest, Detection of transition on model surfaces under cryogenic conditions using temperature sensitive paint, 24th International Congress of the Aeronautical Sciences, ICAS 2004 (2004).
- [5] U. Fey, Y. Egami, R. Engler, High Reynolds Number Transition Detection by Means of Temperature Sensitive Paint, in: 44th AIAA Aerospace Sciences Meeting and Exhibit, American Institute of Aeronautics; Astronautics, 2006. <https://doi.org/10.2514/6.2006-514>.
- [6] C. Klein, U. Henne, Y. Deisuke, V. Ondruss, U. Beifuss, A.-K. Hensch, J. Quest, Application of Carbon Nanotubes and Temperature Sensitive Paint for the Detection of Boundary Layer Transition under Cryogenic Conditions (Invited), in: 55th AIAA Aerospace Sciences Meeting, American Institute of Aeronautics; Astronautics, 2017. <https://doi.org/10.2514/6.2017-0336>.
- [7] C. Klein, D. Yorita, U. Henne, V. Ondrus, A.-K. Hensch, R. Longo, A. Gimbel, S. von Deetzen, Application of Temperature Sensitive Paint to investigate laminar-to-turbulent transition on nacelles, in: AIAA Scitech 2020 Forum, American Institute of Aeronautics; Astronautics, 2020. <https://doi.org/10.2514/6.2020-1608>.
- [8] ETW GMBH, Evaluation of the Benefits of innovative Concepts of laminar nacelle and HTP installed on a business jet configuration, HORIZON 2020 Project (2020). <https://doi.org/10.3030/821048>.
- [9] ETW GMBH, High Speed Wind Tunnel Test of a Laminar Configuration Bizjet, (2015). [https://cordis.europa.eu/docs/results/338/338517/final1-hilambiz-publishable-summary\\_rev3.pdf](https://cordis.europa.eu/docs/results/338/338517/final1-hilambiz-publishable-summary_rev3.pdf).
- [10] P. Guntermann, NLF WingHiPerNLF Wing High Speed Performance Test, Cordis (2015). [https://cordis.europa.eu/docs/results/641/641455/final1-nlf-winghiper\\_sfw-publishable-summary\\_rev2.pdf](https://cordis.europa.eu/docs/results/641/641455/final1-nlf-winghiper_sfw-publishable-summary_rev2.pdf).
- [11] C. Klein, Boundary layer transition detection on wind tunnel models in PETW during continuous pitch traverse, in: AIAA Scitech 2019 Forum, American Institute of Aeronautics; Astronautics, 2019. <https://doi.org/10.2514/6.2019-1180>.
- [12] T. Liu, J.P. Sullivan, K. Asai, C. Klein, Y. Egami, Pressure and Temperature Sensitive Paints, Springer International Publishing, 2021. <https://doi.org/10.1007/978-3-030-68056-5>.
- [13] M. Schäferling, V. Ondrus, The Art of Fluorescence Imaging with Chemical Sensors: The Next Decade 2012–2022, *Chemosensors* 12 (2024) 31. <https://doi.org/10.3390/chemosensors12030031>.
- [14] Y. Egami, U. Fey, C. Klein, J. Quest, V. Ondrus, U. Beifuss, Development of new two-component temperature-sensitive paint (TSP) for cryogenic testing, *Measurement Science and Technology* 23 (2012) 115301. <https://doi.org/10.1088/0957-0233/23/11/115301>.
- [15] V. Ondrus, R.J. Meier, C. Klein, U. Henne, M. Schäferling, U. Beifuss, Europium 1,3-di(thienyl)propane-1,3-diones with outstanding properties for temperature sensing, *Sensors and Actuators A: Physical* 233 (2015) 434–441. <https://doi.org/10.1016/j.sna.2015.07.023>.